CMS Physics Analysis Summary

2009/02/24

Plans for Jet Energy Corrections at CMS

The CMS Collaboration

Abstract

Jet corrections at CMS will initially be derived from simulation tuned on test beam data, determined directly from collision data when available, and ultimately from a simulation tuned on collision data. The corrections will be factorized into a fixed sequence of sub-corrections associated with different detector and physics effects. The following three factors are minimum requirements for most analysis: offset corrections for pile-up and noise; correction for the response of the calorimeter as a function of jet pseudorapidity relative to the barrel; and correction for the absolute response as a function of transverse momentum in the barrel. The required correction gives a jet Lorentz vector equivalent to the sum of particles in the jet cone emanating from a QCD hard collision. The following additional factors will be provided for use if desired by the analysis: dependence on the fraction of jet energy in the electromagnetic calorimeter; dependence on the flavor of the final state jet; removal of underlying event energy; and correction back to the parton level. We discuss the current status of these corrections, the planned data-driven techniques for their derivation, and their anticipated evolution with the stages of the CMS experiment.

1 Introduction

The goal of the jet energy correction is to relate, on average, the jet energy measured in the detector to the energy of the final state particle jet or parton jet. Here we will concentrate on jets reconstructed from calorimeter energy depositions. We note that CMS is also studying jets reconstructed in three other ways: from tracks alone, from calorimeter energy supplemented with track momentum, and from individually reconstructed particles. Many of the techniques we discuss for correcting calorimeter jets are also planned for jets reconstructed in these other ways.

We define the following types of jets: *GenJets*, or particle jets, are made from clusters of colorless stable MC particles; *CaloJets*, or jets at the calorimeter level, are made from clusters of energy deposits in projective calorimeter towers [1]. The underlying calorimeter cells are initially calibrated using particles in a testbeam. Various in-situ calibrations of the calorimeter cells are planned using jets and isolated charged tracks. Despite the underlying calibration of the calorimeter cells, particle level jet energy corrections are still needed to correct the observed CaloJet energy to equal the GenJet energy on average. Parton level jet corrections are optionally used to correct the CaloJet energy to equal the energy of the originating parton on average.

CMS is developing a factorized multi-level jet correction, shown schematically in Fig. 1, in which the correction must be applied in the following fixed sequence:

1. **Offset**: Required correction for pile-up and electronic noise.
2. **Relative (η)**: Required correction for variations in jet response with pseudorapidity relative to a control region.
3. **Absolute (p_T)**: Required correction to particle level versus jet p_T in the control region.
4. **EMF**: Optional correction for variations in jet response with electromagnetic energy fraction.
5. **Flavor**: Optional correction to particle level for different types of jets (light quark, c, b, gluon)
6. **Underlying Event**: Optional correction for underlying event energy due to soft interactions involving spectator partons.
7. **Parton**: Optional correction to parton level.

Figure 1: Schematic picture of the factorized multi-level jet correction, in which corrections to the reconstructed jet are applied in sequence to obtain the final calibrated jet. Required correction levels are shown in solid boxes and optional correction levels are shown in dashed boxes.

If we include only the required jet corrections, an equation relating the corrected CaloJet energy to the uncorrected CaloJet energy is

$$\text{Corrected CaloJet Energy} = (\text{CaloJet Energy} - \text{offset}) \times C(\text{rel:}\eta) \times C(\text{abs:}p_T) \qquad (1)$$

Equation 1, which includes the offset, relative and absolute corrections, can be extended to include the optional corrections by multiplying the right hand side by further correction factors, C(EMF), C(Flavor), C(UE) and C(Parton).

CMS plans to measure many of these corrections directly with in-situ collider data, as was done by the Tevatron experiments [2, 3]. The most common technique is to use conservation of transverse momentum, known as p_T balance, in a $2 \rightarrow 2$ process. Here at least one of the two final state objects is a jet whose response is measured relative to the other final state object which serves as the reference. CMS plans to employ p_T balance in dijet events, photon + jet events, and Z + jet events, to determine jet energy corrections using collider data. All figures in this note are obtained from Monte Carlo simulations of 14 TeV proton-proton collisions using PYTHIA [4] and a full CMS detector simulation based on GEANT4 [5]. CMS is developing jet corrections for the iterative cone algorithm [1], the seedless infrared safe cone algorithm [6], and a K_T algorithm [7]. Unless otherwise stated, the results and figures in this note correspond to jets from the CMS iterative cone algorithm with a cone size $\Delta R = \sqrt{\Delta\eta^2 + \Delta\phi^2} = 0.5$.

2 Offset Correction

Pile-up of multiple proton-proton collisions and electronic noise in the detector produce an energy offset. The goal of the offset correction is to subtract, on average, the unwanted energy from the jet. To estimate the size of the expected energy offset, we use noise-only and minimum-bias MC events. Fig. 2 shows the energy, E, and transverse energy, E_T, collected inside a random cone of radius $\Delta R = 0.5$ as a function of $|\eta|$, separately for simulation of noise and one pile-up event. The results are obtained with the current calorimeter thresholds used

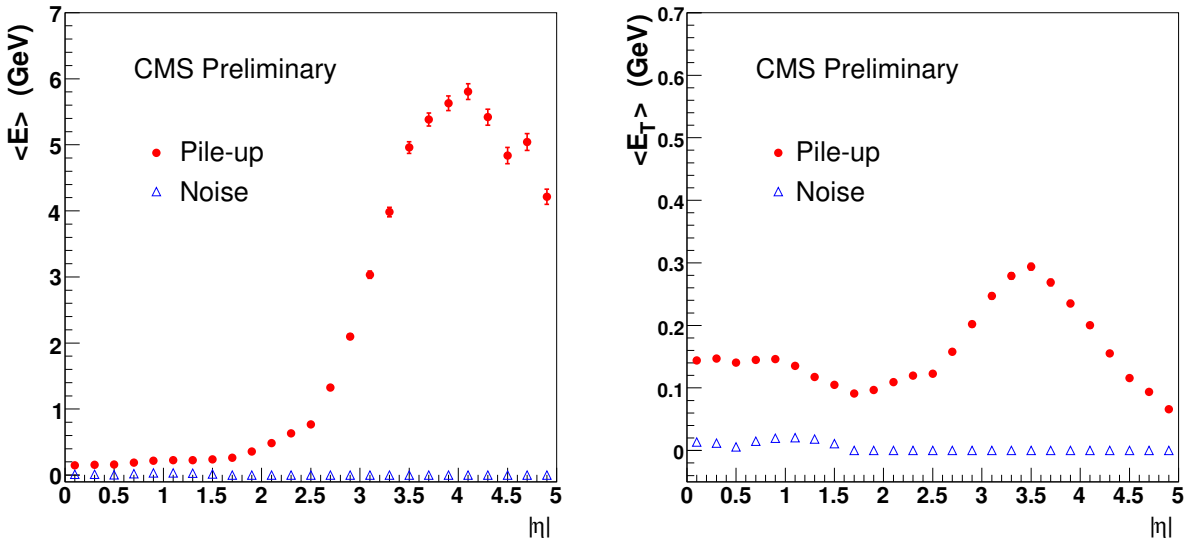

Figure 2: The measured jet energy (left) and transverse energy (right) expected from electronic noise and pile-up of one additional minimum-bias event. Calorimeter cell and tower thresholds have been applied (see text).

for jet reconstruction: scheme B cell thresholds to suppress noise [1], and tower $E_T > 0.5$ GeV to suppress pile-up. Offset due to electronic noise is found negligible with these thresholds. Offset due to a single pile-up event is small: $< E_T > \approx 0.1 - 0.3$ GeV. We expect the offset will

increase roughly proportionally with the number of pile-up events. In collider data, we plan to estimate the energy offset due to noise and pile-up from zero-bias events, which do not require any interaction to trigger, and also minimum-bias triggered events. The offset correction subtracts the energy offset from the measured jet energy.

3 Relative Correction: η dependence

The CMS jet response varies as a function of jet η for a fixed jet p_T. The purpose of the η dependence correction is to remove these variations and make the response flat as a function of η. This will be done after the offset correction. We plan to determine this correction first from MC truth, and later from QCD dijet events in actual collision data applying the p_T balance technique.

3.1 MC Truth Based Corrections

To derive η dependence corrections from MC, we use QCD dijet events. In these events we match CaloJets to GenJets by requiring their separation in $\eta\phi$ space be within $\Delta R < 0.25$. For the matched jets we study the distribution of the variable $\Delta p_T(\eta) = p_T^{CaloJet} - p_T^{GenJet}$ in fine bins of jet η and for various p_T^{GenJet} ranges. To extract the relative jet energy calibration, the most probable value of the $\Delta p_T(\eta)$ distribution in a given η bin is compared to the most probable value of the $\Delta p_T(\eta < 1.3)$ distribution for jets in the control region of the calorimeter, $|\eta| < 1.3$. Fig. 3 shows variations of $p_T^{CaloJet}/p_T^{GenJet}$ as a function jet η, for two different p_T ranges, before and after the relative correction is applied. Before the correction there are significant variations as a function of η. Some of these variations are due to under-response at the edges of the calorimeter sub-systems in η, and other variations are due to over-response in higher η regions where a fixed jet p_T corresponds to a large and varying jet momentum. After the corrections the jet response is flat.

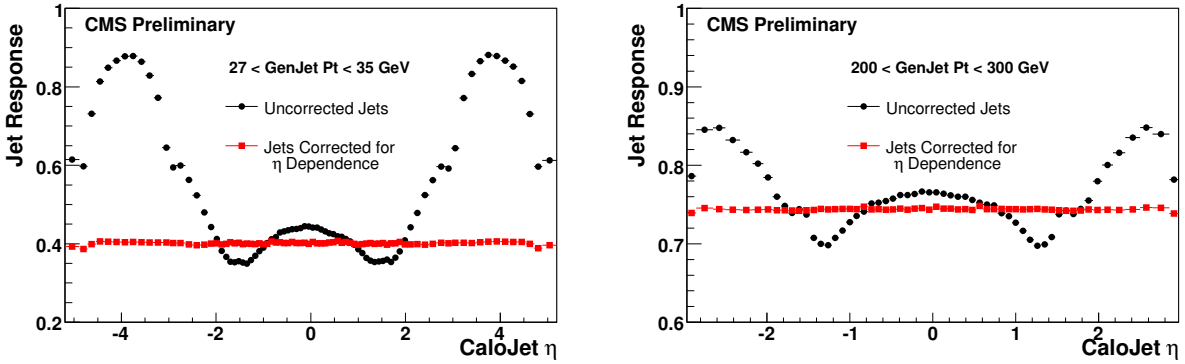

Figure 3: Left) The jet response vs. η from MC truth for GenJets with $27 < p_T < 35$ GeV both before and after η dependent corrections. Right) Same for $200 < p_T < 300$ GeV.

3.2 Data Driven Corrections

To derive the relative jet energy corrections from collider data, we plan to employ the dijet p_T balance technique, first used at SPPS [8] and later refined by the Tevatron experiments [2, 3]. The idea is to use p_T balance in back-to-back dijet events with one jet (barrel jet) in the central

control region of the calorimeter, and the other jet (probe jet) with arbitrary η. To study this method in MC, we use QCD jet events with ≥ 2 jets azimuthally separated by $\Delta\phi > 2.5$. The sample is enriched in the $2 \rightarrow 2$ process by requiring that any additional 3rd jet in the event have $p_T < 0.25 p_T^{dijet}$, where $p_T^{dijet} = (p_T^{probe} + p_T^{barrel})/2$ is an average uncorrected p_T of the dijet system. We study the distribution of the quantity $B = (p_T^{probe} - p_T^{barrel})/2$ in bins of η^{probe} and p_T^{dijet}. The most probable value of the B distribution, <B> in a given η^{probe} and p_T^{dijet} bin is used to determine the relative response R(η^{probe}, p_T^{dijet}) = (2 + <B>) / (2 − <B>). The correction comes from inverting the response and mapping the average p_T^{dijet} to the average p_T^{probe}. Fig. 4 shows the relative jet response as a function of η determined in two ways: from MC truth and from dijet p_T balance. The response values obtained by the two methods agree to within 1% for the barrel ($|\eta| < 1.3$), 2-3% for the endcap ($1.3 < |\eta| < 3$), and 5-10% for the forward ($3 < |\eta| < 5$). The agreement improves when we tighten the cut on $\Delta\phi$ and 3rd jet p_T, nevertheless, we believe this is roughly the size of the systematic uncertainty in the dijet balance technique.

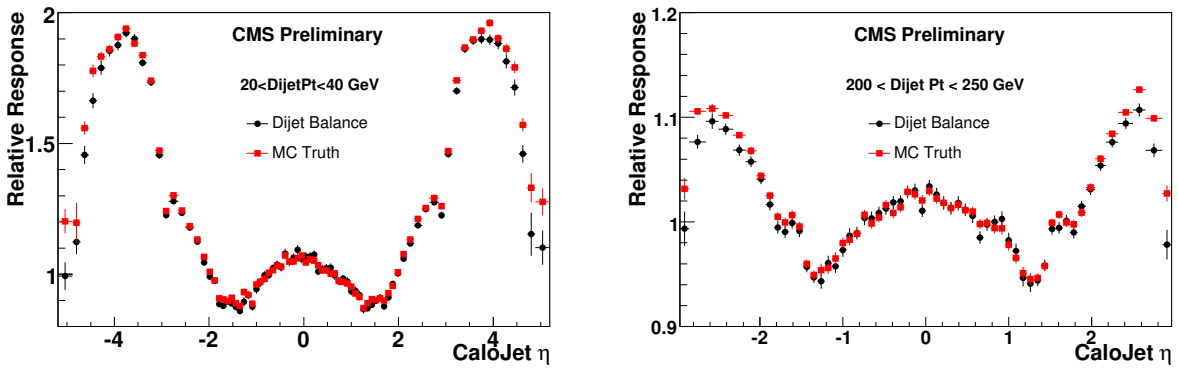

Figure 4: Left) The relative jet response vs. η from both dijet balance and MC truth for $20 < p_T^{dijet} < 40$ GeV. Right) Same for $200 < p_T^{dijet} < 300$ GeV.

4 Absolute Correction: p_T dependence

The CMS calorimeter energy response to a particle level jet is smaller than unity and varies as a function of jet p_T. The purpose of the p_T dependent correction is to remove these variations and make the response equal to unity at all p_T for the control region $|\eta| < 1.3$. When combined with the η dependent correction and the offset correction, the p_T dependent correction provides the complete correction back to the particle jet level required for most CMS analyses. We plan on determining this correction first from MC truth, and subsequently from photon + jet and Z + jet p_T balance in actual collision data.

4.1 MC Truth Based Corrections

To derive p_T-dependence corrections from MC, we use the same QCD dijet events as for the η-dependence studies. The jets are required to be in the central region of the calorimeter, $|\eta_{jet}| < 1.3$ and matched by $\Delta R(GenJet, CaloJet) < 0.25$. The distribution of $\Delta p_T(p_T^{GenJet}) = p_T^{CaloJet} - p_T^{GenJet}$ is studied, and the most probable value $< \Delta p_T >$ is found by a Gaussian fit in the range $\pm 1.5\sigma$ around the peak. The jet response, $R(p_T^{GenJet}) = 1 + < \Delta p_T > / p_T^{GenJet}$, is measured

in bins of p_T^{GenJet}. The jet energy correction is then extracted from $R(p_T^{GenJet})$ by numerical inversion: the correction is $1/R$ expressed as a function of $p_T^{CaloJet}$. Fig. 5 shows both the jet response and the jet correction. To make the calorimeter jet response flat in η and p_T, the CaloJet Lorentz vector is scaled by the product of the η-dependence and p_T-dependence correction factors. This corrects the calorimeter jet (CaloJet) to the particle jet level (GenJet).

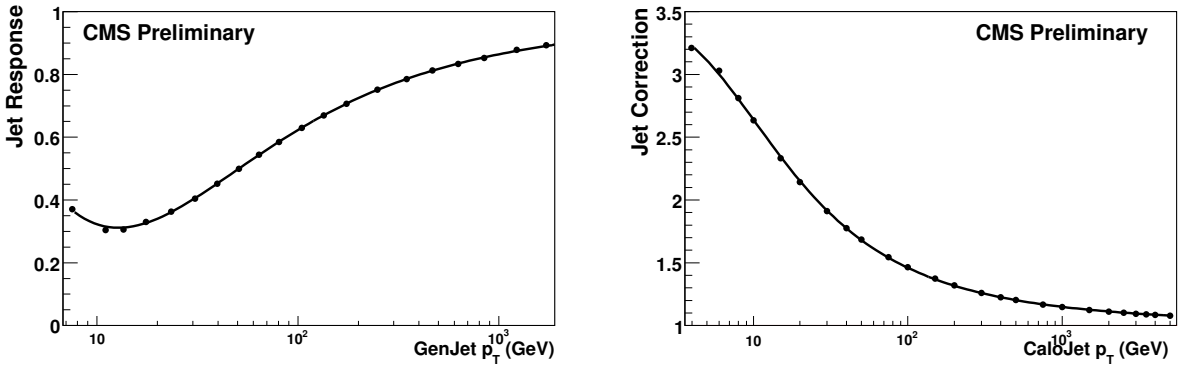

Figure 5: Left) Simulated jet response versus particle jet p_T^{GenJet}. Right) Simulated absolute correction as a function of calorimeter jet $p_T^{CaloJet}$.

4.2 Data Driven Corrections

To determine absolute jet corrections from collider data, we plan to use p_T balance in γ/Z + jet events, with the jet in the control region $|\eta| < 1.3$, a technique introduced by the Tevatron experiments [2, 3]. In the case of γ + jet balance, the γ p_T is measured in the electromagnetic calorimeter (ECAL), which is calibrated using test-beam electrons supplemented with in-situ calibration using $\pi^0 \to \gamma\gamma$, $Z \to e^+e^-$ and $W \to e\nu$. We consider photons reconstructed in the CMS barrel calorimeter, $|\eta^\gamma| < 1.3$. The main background to γ + jet production is QCD dijet events where one jet is misidentified as a photon. To reduce this background we consider only isolated photons. The photon isolation requires minimal activity in the tracker, ECAL and hadronic calorimeter in a cone around the photon candidate. We enhance the fraction of $2 \to 2$ processes by requiring the photon and the leading jet be back-to-back: $|\Delta\phi - \pi| < 0.2$, and by requiring that the second leading jet have small p_T compared to the photon, $p_T^{JET2}/p_T^\gamma < 0.1$. Fig. 6 shows the number of signal and background events expected in an inverse femtobarn after this preliminary set of cuts. The photon signal is larger than the QCD background for $p_T > 100$ GeV. Fig. 6 also shows the expected jet response, p_T^{JET}/p_T^γ, and its expected statistical error with $100pb^{-1}$, demonstrating that with this luminosity we should be able to measure a jet correction up to jet $p_T \sim 600$ GeV.

For Z + jet p_T balance we consider $Z \to \mu\mu$ decays, which do not rely on calorimeter information. The Z p_T will be measured from the μ tracks which reconstruct to the Z mass. We use reconstructed muons with $p_T > 15$ GeV and $|\eta| < 2.3$ and accept events with two muons of opposite charge and a di-muon mass within 20 GeV of the Z mass. We consider only jets that are separated from the muons by $\Delta R > 0.5$. We enhance the fraction of $2 \to 2$ processes by requiring the Z and the leading jet be back-to-back, $|\Delta\phi - \pi| < 0.2$, and by requiring that the second leading jet have small p_T compared to the Z boson, $p_T^{JET2}/p_T^Z < 0.2$. We only consider here the Z signal as backgrounds are expected to be negligible. Fig. 7 shows the expected jet response, p_T^{JET}/p_T^Z, and its statistical error with $100pb^{-1}$, demonstrating that with this lumi-

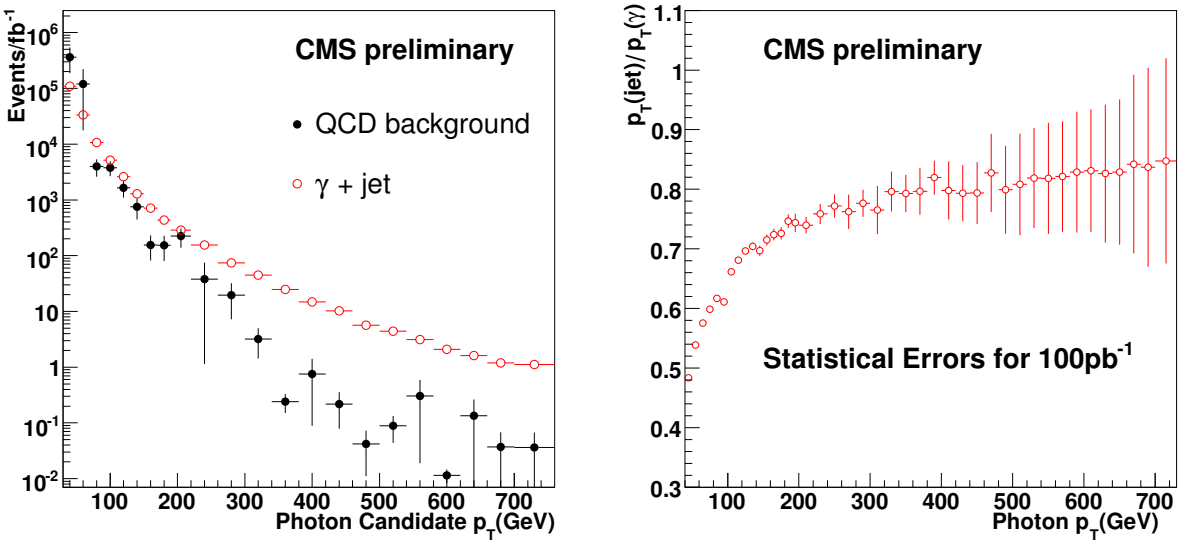

Figure 6: Left) Expected rate of isolated photons and QCD dijet background as a function of photon candidate p_T. Right) The jet response from γ + jet balance with statistical uncertainties anticipated for 100 pb^{-1}.

nosity we should be able to measure a jet correction up to jet $p_T \sim 400$ GeV. The systematic uncertainty in the jet response from the $2 \rightarrow 2$ selection cuts is estimated to be within 2% for all Z p_T.

Deriving the data-driven correction from γ/Z + jet p_T balance requires a few steps. The initial corrections from γ/Z + jet p_T balance come from inverting the response, mapped from a function of $p_T^{\gamma/Z}$ to a function of $p_T^{CaloJet}$. Fig. 7 shows the jet correction from Z +jet p_T balance in comparison to the MC truth correction from the QCD dijet sample. The two corrections are the same to within 5% for $p_T > 100$ GeV, demonstrating that p_T balance can be used to obtain a similar jet correction as MC truth. The small difference between jet response from MC truth for dijets and from γ/Z + jet p_T balance is expected due to two effects. First, in the p_T balance measurements conservation of momentum holds at the parton level, and we are seeing small differences between parton level corrections from p_T balance and particle level jet corrections from MC truth. Parton level corrections are further discussed in section 7. Second, the mix of quarks and gluons recoiling off the γ/Z is different than the mix of quarks and gluons in the QCD dijet sample, and the jet response to quarks and gluons is different for low jet p_T at CMS. These flavor corrections are further discussed in section 6. These effects have been estimated with the Monte Carlo and are small compared to the size of the total correction. We plan to use these MC estimates to transform the initial corrections, that come from γ/Z + jet p_T balance, into jet corrections appropriate for particle level jets originating from the mixture of quarks and gluons in the dijet sample. For example, we plan to take the initial correction derived from Z + jet p_T balance in collider data and multiply it by the curve labeled "MC dijet / $Z + jet$" in Fig. 7, and we plan a similar transformation for the correction derived from γ + jet p_T balance. The data-driven corrections from γ and Z + jet p_T balance can then be combined, weighting by their errors appropriately. The MC truth based corrections from QCD dijets can then be rescaled as necessary to agree with the combined data-driven correction in the p_T regions where they overlap. The rescaled MC truth corrections for QCD dijets will then extrapolate

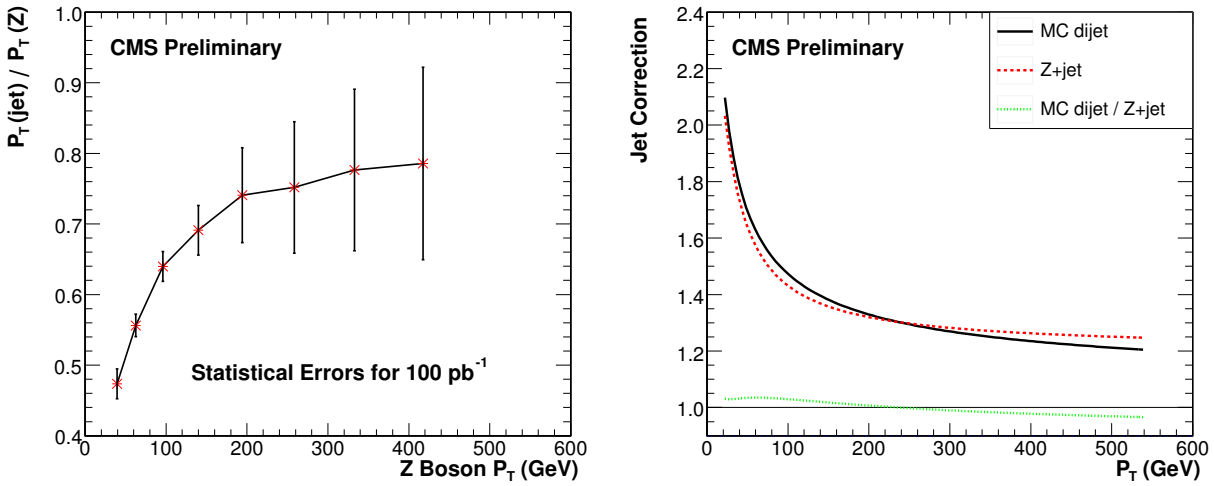

Figure 7: Left) The jet response from Z + jet balance with statistical uncertainties anticipated for 100 pb^{-1}. Right) The jet correction from Z + jet balance, from MC truth for QCD dijets, and the ratio of the two corrections.

the data-driven corrections to the highest and lowest p_T regions where in-situ calibration samples are not available. The result of these steps is the data-driven absolute correction for p_T dependence.

With 100 pb^{-1} of data we expect to be able to use top quark events for data driven corrections [9]. The W mass constraint can give the jet energy correction for light and charm quarks in the rough interval $20 < p_T < 130$ GeV, and the t quark mass constraint can then give the jet energy correction for b quarks in a similar p_T interval. These corrections will then be used as a further constraint on the absolute correction for p_T dependence.

5 EMF Correction

The fraction of the jet energy deposited in the electromagnetic calorimeter (EMF) provides additional information that can be used to improve the jet energy resolution. In Fig. 8 we show that the response of a jet depends on EMF, with significant variations in response at both low and high EMF. Fig. 8 also shows that correcting for response variations with EMF, in addition to the corrections as a function of η and p_T, improves the jet resolution. This is an optional correction, which has been developed from MC truth for CMS analyses requiring optimal jet energy resolution. The data-driven techniques for determining the correction as a function of p_T can also be used to measure the jet response as a function of EMF.

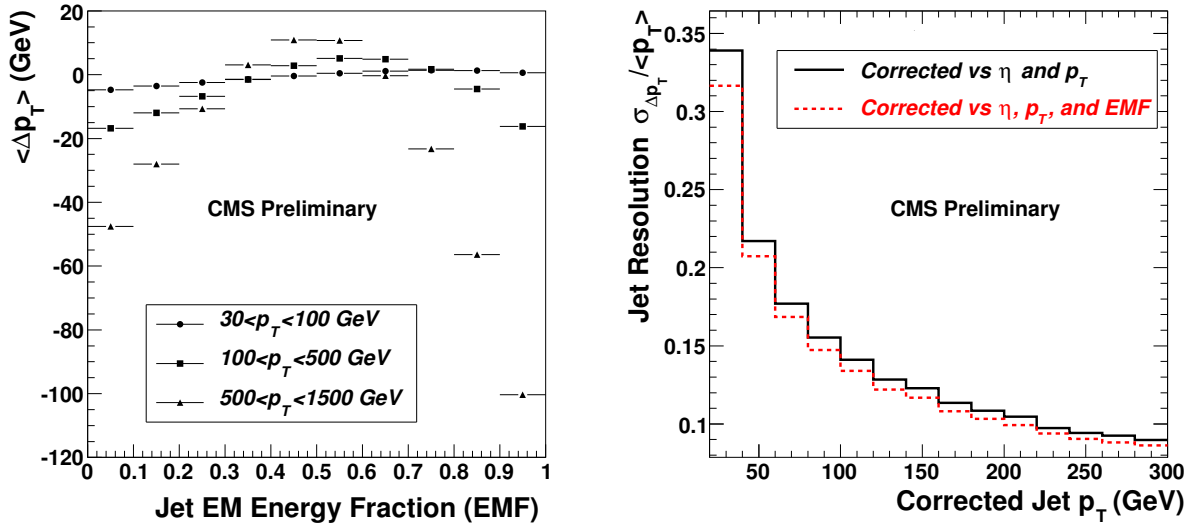

Figure 8: Left) The difference between GenJet p_T and corrected CaloJet p_T is plotted as a function of EMF for three different bins of GenJet p_T. Right) The jet resolution after p_T and η dependent corrections, and after additional EMF dependent corrections.

6 Flavor Correction

The optional flavor correction is intended to correct a jet to the particle level assuming the jet originated from a specific parton flavor, as opposed to the QCD dijet mixture of parton flavors used by the previous corrections. In Fig. 9 we show the jet response variations for different parton flavors. For example, light quarks have higher response than gluons because they fragment into higher momentum particles. Fig. 9 also shows that the QCD dijet mixture is dominated by gluons. Processes like γ/Z + jets, which have a higher fraction of light quarks in the final state, will have a higher jet response. Flavor corrections can be developed from MC truth and from in-situ data samples like $t\bar{t}$ [9]. Analyses which are able to identify the flavor of a jet in the final state, or can assume a specific flavor hypothesis, may benefit from this additional optional correction for jet flavor.

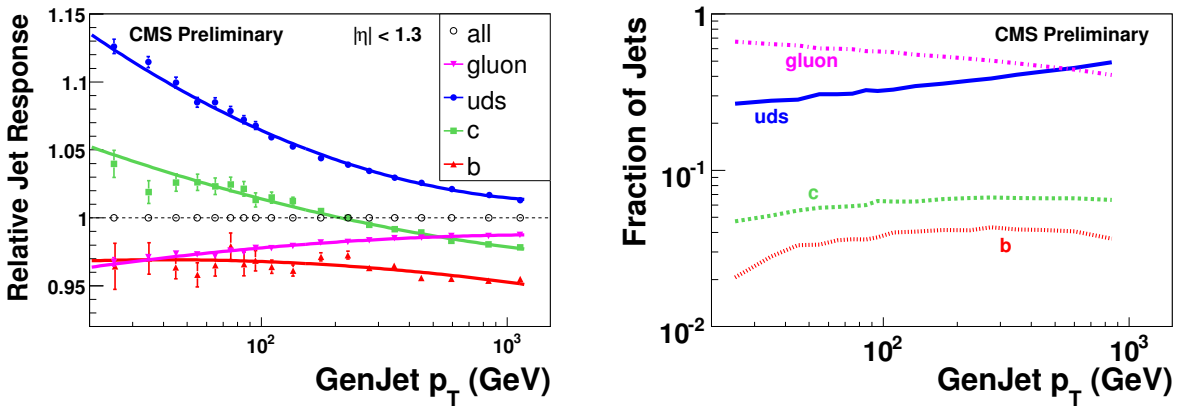

Figure 9: Left) The jet response of gluons, light (uds), c, and b quarks relative to the jet response for the QCD dijet mixture of quarks and gluons (all). Right) The fraction of jets from each flavor in the QCD dijet sample.

7 Parton Correction

The previous corrections take a CaloJet back to the corresponding GenJet on average. The parton correction then takes the jet back to the corresponding parton, on average. Fig. 10 shows the GenJet response to an input parton, $p_T^{GenJet}/p_T^{parton}$, which clearly depends on the parton flavor. Gluons which radiate more than light quarks have a lower GenJet response, because more final state radiation falls outside the jet. The GenJet response in general will depend on the size of the jet. For the cone algorithm the response increases with the cone size, ΔR, and for the K_T algorithm the response increases with the size parameter D. Fig. 10 shows that the cone algorithm with $\Delta R = 0.5$ and the K_T algorithms with $D = 0.4$ will have a similar parton correction. The parton correction can be separated from the underlying event correction, but the underlying event like the offset is expected to be small, and Fig. 10 includes both effects. This optional correction can be determined from Monte Carlo for dijet events, but is model and process dependent.

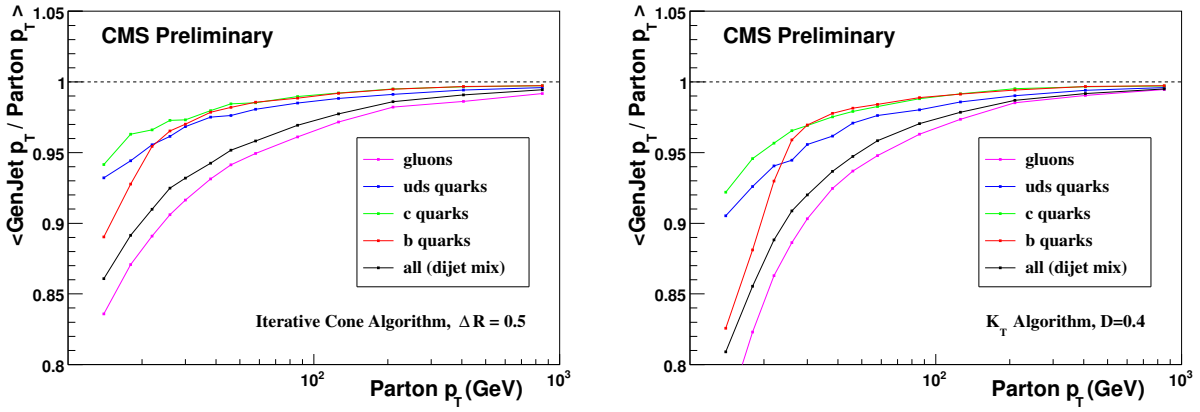

Figure 10: The GenJet response to a parton of different flavors from dijet events for the iterative cone algorithm with cone size $\Delta R = 0.5$ (left) and for the K_T algorithm with $D = 0.4$ (right).

8 Jet Energy Corrections at Startup and Beyond

The procedure of jet energy correction derivation for early periods of data taking is understood to evolve through several cycles. The cycles are driven by underlying calorimeter calibration, availability of adequate statistics for calibration samples, and by the changing accelerator and detector running conditions.

8.1 Calorimeter Workflow

The jet energy correction and its systematic uncertainty depend critically on the underlying calibration of the electromagnetic calorimeter (ECAL) and hadronic calorimeter (HCAL). The in-situ calibration of ECAL uses isolated $\pi \rightarrow \gamma\gamma$ events to achieve uniform azimuthal response. Absolute electromagnetic scale will be derived from $Z \rightarrow e^+e^-$ and $W \rightarrow e\nu$ events. The in-situ calibration of HCAL towers will be performed according to the following scheme:

1. Zero-bias and minimum-bias events will be used to equalize tower-to-tower response in azimuth (ϕ). This will be done separately for each η-ring in the barrel (HB), endcap (HE) and forward (HF) HCAL sub-detectors.

2. Single isolated tracks will be used to calibrate calorimeter towers in HB and HE with respect to the momentum measurement in the tracker ($E_{had}/E_{trk} = 1$).

3. Finally, dijet events will be used to achieve the tower response uniformity in η. The procedure, which employs jets with low fraction of energy deposition in the ECAL detector (EMF$<$0.1), provides tower calibration constants for HE and HF sub-detectors. When done with MC samples, the tower energy correction factor of $\sim$0.7 is obtained for HF.

8.2 Jet Energy Correction Workflow

We envisage the following procedural steps in producing jet energy corrections at CMS

1. We derive MC truth based jet energy corrections to be applied to the earliest data. An effort will be made to keep the MC simulation as realistic as possible. In particular, any modifications in high voltage settings/gains, zero suppression and noise, shall be propagated into the MC simulation to produce the specific samples for derivation of jet energy corrections.

2. We do not include jet energy corrections in the jet triggers. We note that the observed large jet response variation in η, as seen in Fig. 3, has important implication for triggering on jets: the same threshold applied to the uncorrected jet p_T in the level 1 and High Level Trigger corresponds to very different corrected values in different sub-detector regions. Thus, when triggered on uncorrected jet p_T, and given the sharply falling p_T spectrum of the QCD jet production, vastly different jet trigger rates are expected in e.g. the HF sub-detector compared to the HB. Thus it is important to take out the calorimeter response η non-uniformity already at the triggering stage. At the same time, care needs to be taken in order not to introduce large biases in distributions of jets, which could prove to be difficult to correct later at the analysis stage. Therefore we plan to apply a simple factor of 0.7, as determined from MC, to HF towers at the triggering stage. We will also take a few fills without any correction factors applied to the calorimeter towers to have a control sample of raw data with which we can study any possible biases.

3. The calibration procedure described in section 8.1 will be performed to extract HCAL tower-to-tower calibrations and ECAL calibrations from data. These then will be used to re-process the data. The MC samples shall also be reprocessed with the new calibration constants obtained through an equivalent calibration procedure.

4. The effort to derive jet energy corrections from data will proceed in parallel to the calorimeter calibration work in step 3 above, using the data samples with the original calibration values. MC truth jet corrections will be replaced by data-driven values once the samples with adequate statistics are analyzed for extracting jet energy corrections. We will introduce the first offset corrections based on zero-bias collision data. We expect that soon after the first jet data is available we will replace the MC truth relative correction for η dependence with a data-driven correction determined from dijet p_T balance. The first data-driven absolute correction for p_T dependence will come next.

5. After re-processed datasets become available with the new calorimeter calibrations, the jet energy corrections will be re-derived for data and MC. Energy corrections for jets in the MC samples will be based on the MC-truth method.

6. The entire chain of jet energy correction derivation beginning at step 4 for data and MC will be repeated periodically. The frequency of the cycles will be driven by changes in the underlying calorimeter calibrations and in the running conditions. The jet energy corrections will also be upgraded for each significant increase in statistics of the calibration samples. We expect that CMS will only go back to step 3 if there is a significant change in the underlying calorimeter calibration, for example due to a change in the gains.

9 Evolution of Corrections and Systematic Uncertainty

Jet corrections at CMS are currently derived from simulation, illustrated by the figures already presented. In this note we have only briefly mentioned Monte Carlo estimates of the systematic uncertainty in these techniques, because the systematic uncertainty will likely be dominated by effects in the real collider data we cannot anticipate in advance. It is the level of agreement we see between different in-situ calibration channels in the real data, and the comparison of the simulation with the same data, that will likely set our systematic uncertainty. CMS has data on the calorimeter response to particle beams between 2 and 300 GeV, which should allow us to control the systematic uncertainty in simulated calorimeter response to jets. We expect from prior HEP experience that a systematic uncertainty of $\sim$10% on the jet energy is achievable initially using simulation tuned on particle beam data. Once collision data is available we plan on using the data-driven techniques discussed in this note to derive the jet energy corrections. Simultaneously we will use this data to constrain the uncertainty in the simulation. We expect that this process will allow us to reduce the systematic uncertainty on the jet energy to $\sim$5%. The long term JES with a target uncertainty of $\sim$1% will probably take significant time and effort to achieve, and will be based on both well understood samples of collider data and a highly tuned data driven simulation.

10 Conclusions

We have presented a plan for developing jet energy corrections at CMS. The experience of prior experiments, especially the Tevatron, has been applied to the CMS environment in developing this plan. The most important feature of the plan is the factorization of the jet energy correction

into a fixed sequence of sub-corrections. We will measure many of the sub-corrections directly from collision data.

References

[1] **CMS** Collaboration, G. L. Bayatian et al., "CMS physics: Technical design report,". CERN-LHCC-2006-001.

[2] **DØ** Collaboration, B. Abbott et al., "Determination of the absolute jet energy scale in the DØ calorimeters," *Nucl. Instrum. Meth.* **A424** (1999) 352–394, arXiv:hep-ex/9805009. doi:10.1016/S0168-9002(98)01368-0.

[3] A. Bhatti et al., "Determination of the jet energy scale at the Collider Detector at Fermilab," *Nucl. Instrum. Meth.* **A566** (2006) 375–412, arXiv:hep-ex/0510047.

[4] T. Sjostrand, S. Mrenna, and P. Skands, "PYTHIA 6.4 physics and manual," *JHEP* **05** (2006) 026, arXiv:hep-ph/0603175.

[5] S. Banerjee, "Readiness of CMS Simulation Towards LHC Startup,". FERMILAB-CONF-07-612-CD, CERN-CMS-CR-2008-003, Nov 2007.

[6] G. P. Salam and G. Soyez, "A practical Seedless Infrared-Safe Cone jet algorithm," *JHEP* **05** (2007) 086, arXiv:0704.0292.

[7] M. Cacciari and G. P. Salam, "Dispelling the N**3 myth for the k(t) jet-finder," *Phys. Lett.* **B641** (2006) 57–61, arXiv:hep-ph/0512210. doi:10.1016/j.physletb.2006.08.037.

[8] **UA2** Collaboration, P. Bagnaia et al., "Measurement of Production and Properties of Jets at the CERN anti-p p Collider," *Z. Phys.* **C20** (1983) 117. doi:10.1007/BF01573214.

[9] **CMS** Collaboration, "Measurement of jet energy scale corrections using top quark events," **CMS Physics Analysis Summary Top-07-004** (May 2008).